Proceedings of the IASS 2024 Symposium
Redefining the Art of Structural Design
August 26-30, 2024, Zurich Switzerland
Philippe Block, Giulia Boller, Catherine DeWolf,
Jacqueline Pauli, Walter Kaufmann (eds.)

Dynamic Relaxation modeling of beam structures with a novel non-unit quaternion formulation

Axel LARSSON*, Sigrid ADRIAENSSENS

*Department of Civil and Environmental Engineering, Princeton University
Princeton University, Princeton, 08544 NJ, United States of America
a.larsson@princeton.edu

Abstract

Dynamic Relaxation (DR) is a method to form-find and analyze structures undergoing large displacements, by forward time integration of nodal accelerations. Applying DR to beam structures is challenging due to the coupling between internal forces and torques, often resulting in slow convergence. Many beam formulations use rotation vectors to represent rotations, which require special time integration schemes to maintain validity. The difficulty in implementing these integrators is a barrier to exploring more sophisticated solution schemes for DR. To address this challenge, we propose a novel non-unit quaternion representation which allows DR for beams to be used with any time integrator in Euclidian space. We demonstrate the validity of our novel formulation on two large geometrically nonlinear example problems with known solutions. The results align with existing literature, indicating that our formulation enables DR of beam elements to be solved using ODE time integrators for Euclidian space. This novel formulation is of interest to designers and modelers of light weight structures and allows for the efficient and correct modeling of for example beam, bending-active and spline-supported membrane or cable structures.

Keywords: dynamic relaxation, form finding, bending active structures, non-unit quaternions.

1. Introduction

An initially straight slender rod, with low bending stiffness, can greatly increase its load bearing capacity by undergoing a large bending displacement [1]. Such bending-active rods can be assembled into Elastic Rod Networks (ERNs), which, depending on their prescribed deformations and external loadings, can exhibit attractive structural behavior such as a high stiffness to span ratio and multistability [2], [3]. These features enable the construction of lightweight structures with many applications across different scales, such as in structural engineering, metamaterials and aerospace engineering. However, the design and analysis of such ERNs present a challenge because of the nonlinear relationship between their deformed shape, external loading, and prescribed displacements [1], [4]. More specifically, to find the shape of an ERN in static equilibrium, we seek a displacement $u^\star$ from an initially unloaded configuration, such that there is a balance between internal forces and moments F_i, and externally applied loads F_e :

$$R(u^\star) = F_i(u^\star) - F_e(u^\star) = 0 \tag{1}$$

Where $R(u)$ is the residual, which may be nonlinear and can in that case often be solved with Newton's method [5]. However, the simulation of the deployment procedure for initially flat ERNs to a fully deployed shape is difficult, due to the ill conditioned tangential stiffness matrix. As a result Newton's method may face slow or no convergence when solving for the deformed shape of an initially flat ERN.

The convergence issues for Newton's method motivates the use of a Dynamic Relaxation (DR) approach where the nonlinear root-finding problem in equation (1) is recast as an ordinary differential equation (ODE), for which a steady state solution is sought. DR and its variations have been employed to simulate

a variety of structural typologies such as cable and membrane structures, and gridshells [6], [7], [8], [9], [10], [11], [12]. When DR is applied to the modeling of beam structures, the coupled translations and rotations frequently leads to slow convergence for explicit methods [4], leading to a significantly higher computational cost than when DR is applied to cable or truss structures with only translational degrees of freedom.

There are different strategies for mitigating this issue. For instance, the choice of mass matrix can lower the stiffness matrix condition number [13]. Another approach is to choose a beam element representation that does not use rotational degrees of freedom, for instance a nonlinear finite element formulation [14], or a simplified model where the bending and torsional moments are finite difference approximated as shear forces [4], [15]. Throughout many scientific fields, higher order time integrators with favorable stability properties are used to solve for the steady state of stiff ODEs [16], [17]*(NB. that "stiff" has a different meaning in the context of differential equations than in structural engineering, see [18]).* However, many of the time integrators in readily available open source libraries are formulated for state variables in Euclidian space. This makes them unsuitable in unmodified form for DR with many common beam discretizations, whose the rotational degrees of freedom are not in Euclidian space [4], [8], [9], [10], [11], [12], [19], [20]. Thus the lack of DR formulations with rotations in Euclidian space hinders the application of state-of-the-art ODE solvers to form find ERNs.

A previous study [21] presented a Geometrically Exact Beam Theory (GEBT) discretization where the rotations were represented by unit quaternions, which can represent rotations on a Euclidian manifold. This is an important contribution as it allows for readily available advanced ODE solvers to be used for DR. However, the use of unit quaternions requires a computationally expensive renormalization for every time step [22].

In this paper, we build upon previous work [21], [23] and employ a computationally efficient co-rotational formulation for the beam discretization. A different co-rotational formulation for 3D-beams using unit quaternions was developed in [24], however, it was not applied to DR. We represent our rotations using non-unit quaternions, which avoid the costly renormalization step associated with unit quaternions. Our implementation is fully compatible with the comprehensive DifferentialEquations.jl framework for ODE solving [17], which allows us to apply numerous proven ODE solvers for DR of ERNs. Implicit ODE solvers are supported through sparse automatic differentiation. We validate our novel DR formulation on two geometrically nonlinear example problems with known analytical solution and find the results to agree both with theory and with previous studies [4], [9]. Ultimately, having access to a vast number of cutting-edge ODE solvers makes it possible to draw benefit from the ongoing development of differential equation solvers without having to reimplement them to integrate rotations.

2. Method

This section briefly outlines the problem of finding the equilibrium shape of elastic rod networks and its computational challenges. Frequently the equilibrium shape of a mechanically nonlinear structure can be solved using Newton's method, but when simulating the deployment of a bending active ERN from an initially flat configuration, a DR method is preferred. After outlining the motivation for DR, we present our novel non-unit quaternion based formulation and its governing equations.

2.1. ERN equilibrium equation

When dealing with bending active structures, which gain stiffness from a large displacement, the equation for static equilibrium equation (1). is frequently nonlinear and would in most cases be solved by Newton's Method [5], which performs the following iterations of $u^\star$, starting from an initial guess ${u_0}^\star$

$$ {u_{i+1}}^\star = {u_i}^\star - \left(K_R({u_i}^\star)\right)^{-1} \cdot R({u_i}^\star) \tag{2} $$

Where $\boldsymbol{K_R}({u_i}^\star)$ is the tangential stiffness matrix (the Jacobian) of the system. Equation (1) may have multiple solutions, which is the case for the elastica curve (see section 3.2), which in two dimensions

has two stable and one unstable equilibrium [25]. At the initial unstable equilibrium, the tangential stiffness matrix of the elastica is singular, and thus non-invertible, meaning that Newton's method cannot be used to solve for the equilibrium state. This issue can be resolved by applying a small initial trigger load that "pushes" the system in the direction of one of the stable equilibria. However, $\boldsymbol{K_R}(u_i^\star)$ will often be ill conditioned (near singular) and pose significant convergence problems for Newton's method [5].

2.2. Dynamic Relaxation formulation

Since bending-active ERN often are deployed from an initially flat configuration, it is desirable to model them with the flat state as an initial guess. This can be accomplished with DR, which solves a dynamics problem associated to equation (1). The dynamics problem is a second order ODE formulated using Newton's second law. This ODE can in turn be reformulated as a system of first order ODEs:

$$\begin{aligned} \frac{du}{dt} &= v \\ \frac{dv}{dt} &= M^{-1}R(u) \\ u(0) &= u_0 \end{aligned} \tag{3}$$

Where $u = u(t)$ is the displacement at $t \in (0, \infty)$, $v(t)$ is the velocity, M is the system mass matrix and u_0 is an initial displacement. We discretize the system using co-rotational beam elements following [4], [8], [9], with the modification that we calculate the internal bending and twisting moments at each node by applying non-unit quaternion rotations [23] to the local beam coordinate systems. The degrees of freedom for a node node $\boldsymbol{u_i}$ is described by four sub-vectors:

$$\boldsymbol{u_i} = \begin{bmatrix} \boldsymbol{x_i} \\ \boldsymbol{q_i} \\ \boldsymbol{v_i} \\ \boldsymbol{\omega_i} \end{bmatrix} \tag{4}$$

Where $\boldsymbol{x_i} \in R^3$is the translational components of node $\boldsymbol{u_i}$ and $\boldsymbol{q_i} = [a_i, b_i, c_i, d_i]^T$ refers to the four quaternion components describing the nodal rotation. The translational and rotational velocities are denoted $\boldsymbol{v_i} \in R^3$ and $\boldsymbol{\omega_i} \in R^3$ respectively. Thus each node has 13 degrees of freedom in total. The governing equations at the node level can be stated as:

$$\begin{aligned} \frac{d\boldsymbol{x_i}}{dt} &= \boldsymbol{v_i} \\ \frac{d\boldsymbol{q_i}}{dt} &= \frac{1}{2}\boldsymbol{\Omega q_i} + c\boldsymbol{q_i} \\ \frac{d\boldsymbol{v_i}}{dt} &= M^{-1}R^f{}_i(\boldsymbol{u}) \\ \frac{d\boldsymbol{\omega_i}}{dt} &= J^{-1}(R^m{}_i(\boldsymbol{u}) - \boldsymbol{\omega_i} \times J\boldsymbol{\omega_i}) \\ \boldsymbol{u_i}(0) &= \boldsymbol{u_{0i}} \end{aligned}$$

$$\Omega = \begin{bmatrix} 0 & -\omega_1 & -\omega_2 & -\omega_3 \\ \omega_1 & 0 & \omega_3 & -\omega_2 \\ \omega_2 & -\omega_3 & 0 & \omega_1 \\ \omega_3 & \omega_2 & -\omega_1 & 0 \end{bmatrix} \tag{5}$$

Here $R^f{}_i$ and $R^m{}_i$ are the force and torque resultants at node i, respectively. $J \in \mathbb{R}^{3x3}$ is the moment of inertia matrix, and $\boldsymbol{u_{0i}} \in \mathbb{R}^{13}$ is a prescribed initial condition. $c = k(1 - \boldsymbol{q^T q})$ where k is a scalar, typically set to 0.01 [20], and $0 \leq \alpha \leq 1$ is a scalar viscous damping term to reduce solution oscillations. We solve the ODE by integrating forward in time until a steady state is reached. Typically, the solving process is terminated once the force residual norm is below a given tolerance tol. The choice of ODE time solver is a trade off between accuracy, stability, computational expense for each solver step, and the number of steps required to reach convergence. Previous DR beam implementations have employed explicit solvers [4], [9], [10] that only depend on the function evaluated at current state vector, or implicit solvers [19], [20], which depend on the function value evaluated at the next state. However, a great deal of higher order and unconditionally stable ODE solvers (e.g. [16]) have yet to be explored in DR applications. Our DR formulation is compatible with any ODE solver formulated in Euclidian space, which facilitates the application of advanced ODE solvers to DR.

2.3. Implementation

We implement the beam discretization in the Julia programming language[26]. Our program interfaces to the comprehensive DifferentialEquations.jl ODE solver suite [17] for time integration of equation 5.

3. Results

To validate our DR formulation, we solve two large displacement beam problems with known analytical solutions. Those are: 1) a cantilever rod with an applied end moment (section 3.1) and 2) the elastica buckling problem (section 3.2). Although these problems are typically stated in two dimensions, we solve the problems in three dimensions.

In both example problems, we consider a slender beam with isotropic linear elastic material of length L = 10m and following [4], [9] we choose bending stiffness $EI = 10^5 Nm^2$ and axial stiffness $EA = 10^8 N$. For time integration, we choose the *TR-BDF2* solver [27], which has been shown to have high accuracy for 2D structural dynamics problems [28]. For both examples, we note the dependency of the relative error of the number of subdivisions. To avoid oscillatory solutions, we add a callback function to multiply the translational and rotational velocities by a decay factor $c = 0.99$, at a constant rate set to be two times the initial time step guess, i.e.

$$\boldsymbol{v_i}(\mathrm{t}) = \begin{matrix} c * \boldsymbol{v_i}, (t \bmod dt_0) = 0 \\ \boldsymbol{v_i}, (t \bmod dt_0) \neq 0 \end{matrix} \tag{6}$$

And similarily for the rotational velocities.

3.1. Cantilever with end moment

A materially linear elastic cantilever beam subjected to a constant moment M will bend to the shape of a circular curve, according to the equation $M = \frac{EI}{r}$, where r is the curvature radius of the curve and EI

is the bending stiffness of the rod [23]. When $r = \frac{L}{2\pi} \Longrightarrow M = \frac{2\pi EI}{L}$, the beam assumes the shape of a circle, see figure 1.

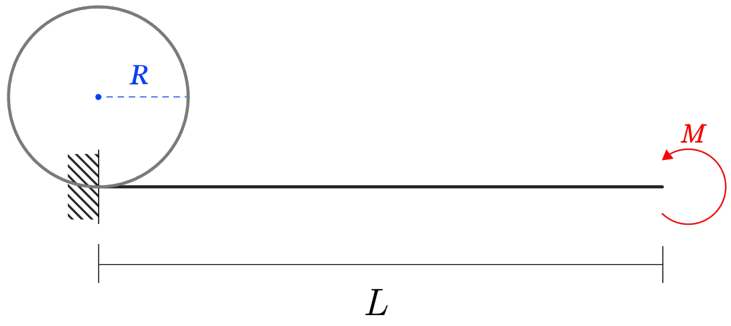

Figure 1: Cantilever beam loaded with end moment *M*. Initial shape shown in black and equilibrium shape shown in gray for $M = \frac{2\pi EI}{L}$.

Using our formulation, we uniformly discretize the beam with a number of elements, *n*, and solve the cantilever moment problem *TR-BDF2*. The viscous damping term $\alpha = 0.99$. We use adaptive timestepping with the initial guess for the time step $dt = 0.1$ and solve with DR until the norm of the residual is smaller than the tolerance $tol = 10^{-6}N$, when the solution is assumed to have converged. Figure 2 shows the DR results as a function of the number of elements *n*. As *n* increases, the DR simulation more closely approximates the analytical curve shape.

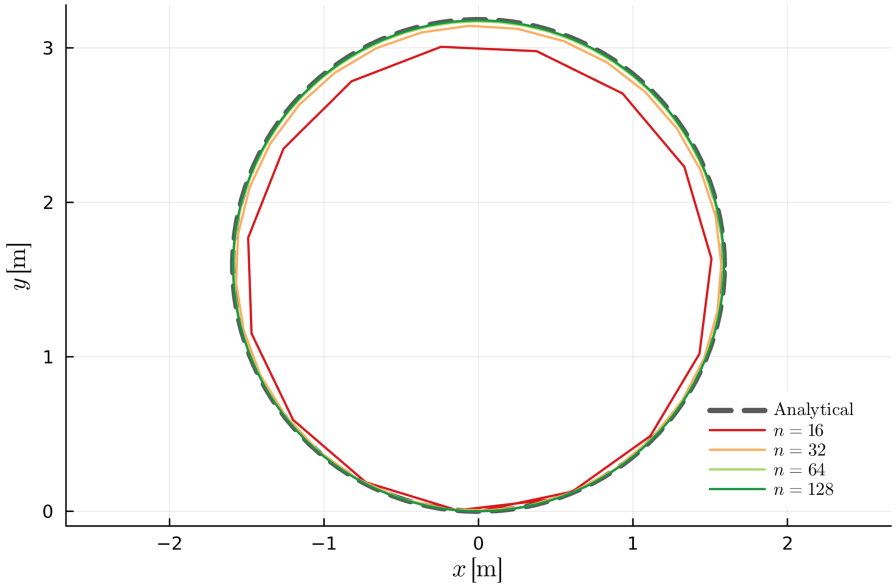

Figure 2: DR results for the cantilever example with $M = \frac{2\pi EI}{L}$. The number of elements is denoted by *n*.

This trend can also be observed in table 1., which lists the predicted radius, r_{pred} as a function of the number of elements along with their corresponding relative error $\delta(r_{pred}) = \frac{|r_{pred} - r_{true}|}{|r_{true}|}$, with r_{true} being the analytical solution for the radius.

n	r_{pred} [m]	$\delta(r_{pred})$ [%]

16	1.501	5.703
32	1.570	1.355
64	1.585	0.388
128	1.589	0.155

Table 1: Predicted radius and relative error as a function of n for $M = \frac{2\pi EI}{L} \implies r_{true} \approx 1.592\, m$

Many common rotation representations, such as Euler angles or rotation vectors, displays singularities which makes it difficult to represent larger rotations. Quaternion-based representations however, are singularity free [22]. This is illustrated in figure 3, where we present the results of a DR solve where we multiply the applied moment with a scaling factor f to control the number of loops, e.g. f =1.0 corresponds to a single loop, f = 2.0 corresponds to a double loop etc.. The number of elements n was kept constant at n = 128, and the other parameters were kept the same as in the one-loop case. The relative errors for the multi-loop experiment are provided in table 2. Our formulation is clearly able to represent rotations even up to four loops without issues with singularities.

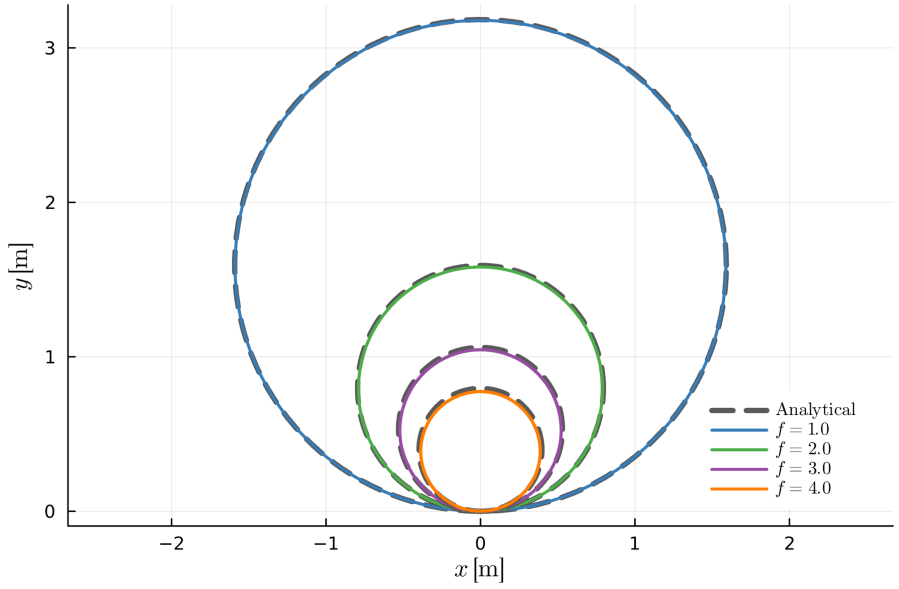

Figure 3: DR results for the cantilever example with $M = f \cdot \frac{2\pi EI}{L}$ and n = *128*.

Scaling factor f	r_{true}[m]	r_{pred} [m]	$\delta(r_{pred})$ [%]
1.0	1.592	1.589	0.155
2.0	0.796	0.791	0.612
3.0	0.531	0.520	1.389

4.0	0.398	0.388	2.510

Table 2: Predicted radius and relative error as a function of f for $M = f \cdot \frac{2\pi EI}{L}$

3.2. Elastica

When a slender rod constrained within a plane, whose endpoints are hinged and constrained to move along a line, is subjected to two opposing point loads larger than the critical buckling load, the rod will buckle out with height y, as shown in figure 4.

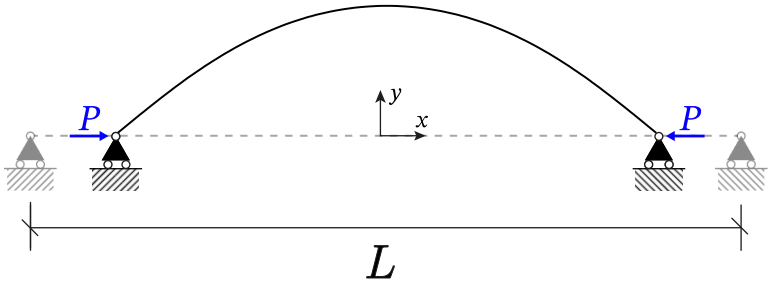

Figure 4: Elastica problem. Two opposing point loads applied to a pinned rod on roller supports causes the rod to buckle out of plane with height y.

Characterizing the post-buckled rod shape is known as the *elastica problem* and has been the subject of centuries of research [30]. We use DR to simulate buckled rod shape according to the previous studies [4], [9]. We consider four load cases, where the opposing loads have magnitude P = 10.48kN, 12.67kN, 18.46kN and 39.48kN. In order to activate the buckling, a small vertical load of size 1N is applied at the beam midpoint. For the first three load cases, we solve the elastica problem with DR using the *TR-BDF2* solver, and solver tolerance $tol = 10^{-6}N$, like in the moment cantilever case. The results of these first three load cases for increasing n are shown in Figure 5. The fourth load case failed to converge for the same solver tolerances. Instead we solved the fourth load case with a tolerance $tol = 1N$ and an initial guess of dt = 10^{-5}. The results for the fourth load case is shown separately in figure 6.

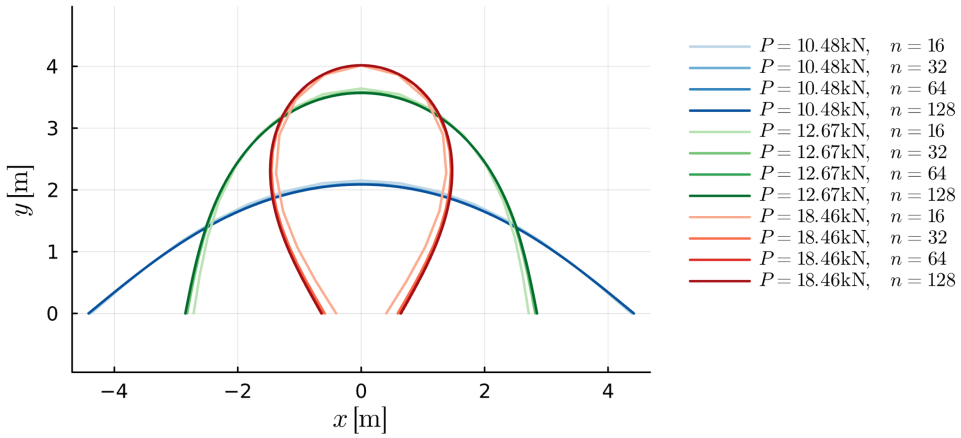

Figure 5: Convergence of DR solutions for the elastica problem with increasing n, for P = 10.48kN, 12.67kN and 18.46kN.

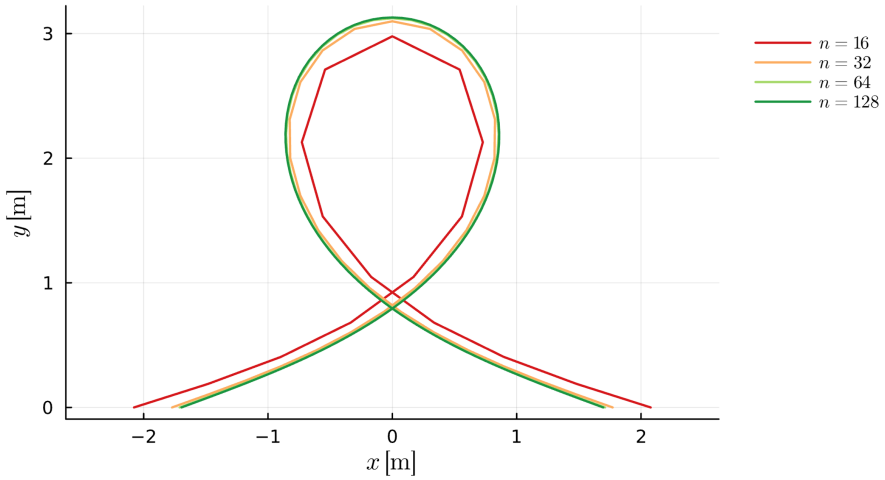

Figure 6: Convergence of DR solutions for the elastica problem with increasing *n,* for P = 39.48kN.

The DR results are collectively presented in table 3, with the column for the fourth load case in gray, to highlight that it was obtained with different solver settings than for the other load cases. The relative errors compared to the analytical solution are shown in table 4. These results are well in agreement with previous studies (compare for instance table 4, with the previous studies shown in table 5 and 6). The general trend is that the relative error decreases significantly between n = 16 and n = 32, but no significant error decrease is seen for higher values of n.

	P = 10.48 kN		P = 12.67 kN		P = 18.46 kN		P = 39.48 kN	
	x/L	y/L	x/L	y/L	x/L	y/L	x/L	y/L
Analytical	0.441	0.211	0.280	0.360	0.062	0.402	-0.170	0.313
N = 16	0.438	0.215	0.272	0.364	0.041	0.402	-0.208	0.298
N = 32	0.441	0.210	0.282	0.359	0.059	0.402	-0.177	0.310
N = 64	0.442	0.209	0.284	0.358	0.063	0.402	-0.171	0.312
N = 128	0.441	0.209	0.285	0.357	0.064	0.402	-0.170	0.313

Table 3: Predicted quantities $\frac{x}{L}$ and $\frac{y}{L}$ for DR solutions of the elastica problem with our formulation.

	P = 10.48 kN		P = 12.67 kN		P = 18.46 kN		P = 39.48 kN	
	$\delta\,(^{x}/_{L})$	$\delta\,(^{y}/_{L})$	$\delta\,(^{x}/_{L})$	$\delta\,(^{y}/_{L})$	$\delta\,(^{x}/_{L})$	$\delta\,(^{y}/_{L})$	$\delta\,(^{x}/_{L})$	$\delta\,(^{y}/_{L})$
N = 16	0.570	2.023	3.021	1.286	34.050	0.079	22.220	4.699
N = 32	0.128	0.348	0.707	0.249	3.890	0.002	4.218	0.835
N = 64	0.293	0.920	1.585	0.624	3.099	0.078	0.635	0.051
N = 128	0.334	1.063	1.801	0.718	4.817	0.076	0.231	0.139

Table 4: Relative error of DR solutions of the elastica problem with our formulation.

4. Discussion and conclusion

The results provide a convincing argument for the validity of our DR formulation. We see that for the moment cantilever example, the relative error of the predicted radius decreases as the number of elements increases. Furthermore, we note that our quaternion-based rotation parameterization is able to represent and accurately model a rod that is looped multiple times in on itself. In the case of the elastica, we demonstrate that our novel implementation can be applied to solve the elastica problem with high solver tolerances, except for in the load case with the larger endpoint load of 39.48 kN, in which a lower tolerance is needed for convergence. However, the relative error for our method is found to be similar across all load cases compared to the previous studies [4], [9] (tables 5 and 6 provided in the appendix A, respectively).

We note that for the elastica problem, the error does not converge in the same manner that the end cantilever moment problem does, despite being solved with identical solver settings for the first three load cases. This phenomenon can also be found in [4], [9]. A possible source of the non-decreasing relative error could be the shortcoming of the method to calculate the beam internal forces and torques which is shared between our formulation and studies [4], [9]. However, further research is required to properly investigate this matter.

Acknowledgements

This research was partially funded by the U.S. National Science Foundation Grant award number 2122269. The authors thank Prof. Francesco Marmo for valuable discussions on the DR method and Dr. Jens Olsson for help in verifying the implementation.

Appendix A1: Relative errors for the elastica problem from previous studies

	P = 10.48 kN		P = 12.67 kN		P = 18.46 kN		P = 39.48 kN	
	$\delta\,(^{x}/_{L})$	$\delta\,(^{y}/_{L})$	$\delta\,(^{x}/_{L})$	$\delta\,(^{y}/_{L})$	$\delta\,(^{x}/_{L})$	$\delta\,(^{y}/_{L})$	$\delta\,(^{x}/_{L})$	$\delta\,(^{y}/_{L})$
N = 16	0.726	2.559	3.821	1.613	40.490	0.025	26.350	5.536
N = 32	0.068	0.190	0.464	0.139	5.691	0.075	5.118	1.024
N = 64	0.272	0.853	1.464	0.584	2.439	0.075	1.000	0.128

Table 5: Relative errors of DR solutions from the study in [4]

	P = 10.48 kN		P = 12.67 kN		P = 18.46 kN		P = 39.48 kN	
	$\delta\,(^{x}/_{L})$	$\delta\,(^{y}/_{L})$	$\delta\,(^{x}/_{L})$	$\delta\,(^{y}/_{L})$	$\delta\,(^{x}/_{L})$	$\delta\,(^{y}/_{L})$	$\delta\,(^{x}/_{L})$	$\delta\,(^{y}/_{L})$
N = 16	0.568	1.943	3.000	1.280	33.980	0.000	22.240	4.704
N = 32	0.159	0.474	0.7143	0.2503	4.065	0.075	4.235	0.832
N = 64							0.647	0.064

Table 6: Relative errors of DR solutions from the study in [9]

References

[1] J. Lienhard, “Bending-active structures: form-finding strategies using elastic deformation in static and kinetic systems and the structural potentials therein,” 2014.
[2] C. Baek, A. O. Sageman-Furnas, M. K. Jawed, and P. M. Reis, “Form finding in elastic gridshells,” *Proc. Natl. Acad. Sci.*, vol. 115, no. 1, pp. 75–80, Jan. 2018, doi: 10.1073/pnas.1713841115.
[3] T. Yu, L. Dreier, F. Marmo, S. Gabriele, S. Parascho, and S. Adriaenssens, “Numerical modeling of static equilibria and bifurcations in bigons and bigon rings,” *J. Mech. Phys. Solids*, vol. 152, p. 104459, Jul. 2021, doi: 10.1016/j.jmps.2021.104459.
[4] S. M. L. Adriaenssens and M. R. Barnes, “Tensegrity spline beam and grid shell structures,” *Eng. Struct.*, vol. 23, no. 1, pp. 29–36, Jan. 2001, doi: 10.1016/S0141-0296(00)00019-5.
[5] P. Deuflhard, *Newton Methods for Nonlinear Problems: Affine Invariance and Adaptive Algorithms*, vol. 35. in Springer Series in Computational Mathematics, vol. 35. Berlin, Heidelberg: Springer Berlin Heidelberg, 2011. doi: 10.1007/978-3-642-23899-4.
[6] M. R. Barnes, “Form Finding and Analysis of Tension Structures by Dynamic Relaxation,” *Int. J. Space Struct.*, vol. 14, no. 2, pp. 89–104, Jun. 1999, doi: 10.1260/0266351991494722.
[7] S. Adriaenssens, M. Barnes, R. Harris, and C. Williams, “Dynamic relaxation: Design of a strained timber gridshell,” in *Shell Structures for Architecture*, Routledge, 2014, pp. 103–116.
[8] C. Brandt-Olsen, “Calibrated Modelling of Form-active Structures,” *TU Den.*, 2016.
[9] J. Olsson, “Implementation of beam elements and size optimization in real time form finding using dynamic relaxation,” p. 97.

[10] E. Poulsen, "Structural design and analysis of elastically bent gridshells-The development of a numerical simulation tool," 2015.
[11] J. Li and J. Knippers, "Rotation formulations for dynamic relaxation—with application in 3D framed structures with large displacements and rotations," *Seoul Sn*, 2012.
[12] G. Senatore and D. Piker, "Interactive real-time physics," *Comput.-Aided Des.*, vol. 61, pp. 32–41, Apr. 2015, doi: 10.1016/j.cad.2014.02.007.
[13] M. Rezaiee-Pajand, S. R. Sarafrazi, and H. Rezaiee, "Efficiency of dynamic relaxation methods in nonlinear analysis of truss and frame structures," *Comput. Struct.*, vol. 112–113, pp. 295–310, Dec. 2012, doi: 10.1016/j.compstruc.2012.08.007.
[14] M. R. Gosz, *Finite Element Method: Applications in Solids, Structures, and Heat Transfer*, 1st ed. CRC Press, 2017. doi: 10.1201/9781315275857.
[15] M. R. Barnes, S. Adriaenssens, and M. Krupka, "A novel torsion/bending element for dynamic relaxation modeling," *Comput. Struct.*, vol. 119, pp. 60–67, Apr. 2013, doi: 10.1016/j.compstruc.2012.12.027.
[16] L. F. Shampine and M. W. Reichelt, "The MATLAB ODE Suite," *SIAM J. Sci. Comput.*, vol. 18, no. 1, pp. 1–22, Jan. 1997, doi: 10.1137/S1064827594276424.
[17] C. Rackauckas and Q. Nie, "DifferentialEquations.jl – A Performant and Feature-Rich Ecosystem for Solving Differential Equations in Julia," *J. Open Res. Softw.*, vol. 5, no. 1, 2017, doi: 10.5334/jors.151.
[18] E. Hairer and G. Wanner, *Solving Ordinary Differential Equations II*, vol. 14. in Springer Series in Computational Mathematics, vol. 14. Berlin, Heidelberg: Springer Berlin Heidelberg, 1991. doi: 10.1007/978-3-662-09947-6.
[19] M. Aguirre and S. Avril, "An implicit 3D corotational formulation for frictional contact dynamics of beams against rigid surfaces using discrete signed distance fields," *Comput. Methods Appl. Mech. Eng.*, vol. 371, p. 113275, Nov. 2020, doi: 10.1016/j.cma.2020.113275.
[20] J. Rombouts, G. Lombaert, L. De Laet, and M. Schevenels, "A fast and accurate dynamic relaxation approach for form-finding and analysis of bending-active structures," *Int. J. Space Struct.*, vol. 34, no. 1–2, pp. 40–53, Mar. 2019, doi: 10.1177/0956059919864279.
[21] E. Zupan, M. Saje, and D. Zupan, "Quaternion-based dynamics of geometrically nonlinear spatial beams using the Runge–Kutta method," *Finite Elem. Anal. Des.*, vol. 54, pp. 48–60, Jul. 2012, doi: 10.1016/j.finel.2012.01.007.
[22] F. L. Markley and J. L. Crassidis, *Fundamentals of Spacecraft Attitude Determination and Control*. New York, NY: Springer New York, 2014. doi: 10.1007/978-1-4939-0802-8.
[23] C. Rucker, "Integrating Rotations Using Nonunit Quaternions," *IEEE Robot. Autom. Lett.*, vol. 3, no. 4, pp. 2979–2986, Oct. 2018, doi: 10.1109/LRA.2018.2849557.
[24] S. Grange and D. Bertrand, "Co-rotational 3D beam element using quaternion algebra to account for large rotations: Formulation theory and static applications," *Int. J. Solids Struct.*, vol. 293, p. 112746, May 2024, doi: 10.1016/j.ijsolstr.2024.112746.
[25] A. Magnusson, M. Ristinmaa, and C. Ljung, "Behaviour of the extensible elastica solution," *Int. J. Solids Struct.*, vol. 38, no. 46–47, pp. 8441–8457, Nov. 2001, doi: 10.1016/S0020-7683(01)00089-0.
[26] J. Bezanson, A. Edelman, S. Karpinski, and V. B. Shah, "Julia: A fresh approach to numerical computing," *SIAM Rev.*, vol. 59, no. 1, pp. 65–98, 2017.
[27] M. Hosea and L. Shampine, "Analysis and implementation of TR-BDF2," *Appl. Numer. Math.*, vol. 20, no. 1–2, pp. 21–37, 1996.
[28] L. Bonaventura and M. G. Mármol, "The TR-BDF2 method for second order problems in structural mechanics," *Comput. Math. Appl.*, vol. 92, pp. 13–26, Jun. 2021, doi: 10.1016/j.camwa.2021.03.037.
[29] J. C. Simo and L. Vu-Quoc, "A three-dimensional finite-strain rod model. part II: Computational aspects," *Comput. Methods Appl. Mech. Eng.*, vol. 58, no. 1, pp. 79–116, Oct. 1986, doi: 10.1016/0045-7825(86)90079-4.
[30] R. Levien, "The elastica: a mathematical history".